DOI: 10.1002/ejic.201000872

Synthesis of a [3Fe2S] Cluster with Low Redox Potential from [2Fe2S] Hydrogenase Models: Electrochemical and Photochemical Generation of Hydrogen

Weiming Gao,*[a][‡] Junliang Sun,[b] Mingrun Li,[b] Torbjörn Åkermark,[c] Kristina Romare,[a] Licheng Sun,[d] and Björn Åkermark*[a]

Keywords: Enzyme models / Electrochemistry / Iron / Hydrogenases / Cluster compounds

In the attempted replacement of carbon monoxide by the bis(phosphane) dppv in a dinuclear [2Fe2S] complex, a trinuclear [3Fe2S] complex with two bis(phosphane) ligands was unexpectedly obtained. On protonation, this gave a bridged hydride complex with an unusually low potential for the reduction of protons to molecular hydrogen. The redox potential also appears sufficiently positive for direct electron transfer from an excited $[Ru(bpy)_3]^{2+}$ sensitizer.

Introduction

During attempts to replace the carbonyl ligands of the hydrogenase mimics **1a** and **1b**[1] by *cis*-1,2-bis(diphenylphosphanyl)ethene (dppv), we used Me_3NO to oxidize the CO groups. This is known to give readily released CO_2, which facilitates the introduction of new ligands.[2–4] Much to our surprise, the trinuclear dppv complex **2** was formed as the major product in both cases in approximately 50% yield. On protonation of this complex with strong acids such as HBF_4 or HOTf, hydride **3** was formed, accompanied by approximately 30% of isomer **4** (Scheme 1).

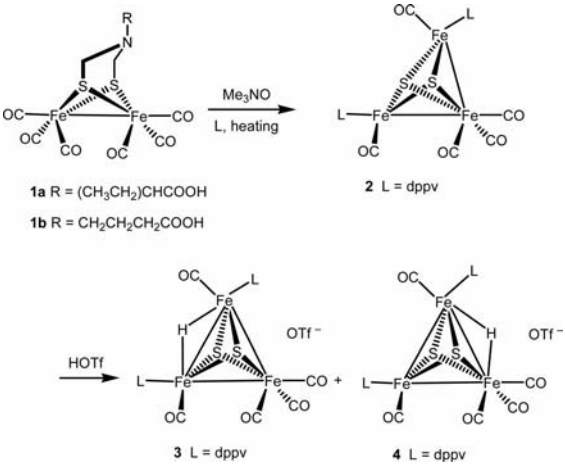

Scheme 1. Formation and protonation of **2**.

Results and Discussion

A tentative mechanism for the remarkable transformation of dinuclear **1** into trinuclear complex **2** first involves catalytic oxidation by Me_3NO of the bridge head nitrogen atoms of **1a** and **1b** to give the corresponding *N*-oxide complexes. As the CO ligands of **1** are replaced by one or two dppv ligands, this oxidation should become more facile. Subsequent Cope rearrangement[5] of the *N*-oxide compounds would then give hydroxylamine derivatives **5**. Complex **5b** (m/z = 1083) could be detected by ESI-MS analysis of the reaction mixture.

Bridge hydrolysis and subsequent hydrosulfide oxidation would then give disulfides **6a**, **6b** and **6c** (Scheme 2). All of these sulfides were detected by ESI-MS analysis of the reaction mixture, and compound **6a** could be isolated in approximately 5% yield. Subsequent reaction between disulfides **6** and excess dppv ligand would afford monosulfides **7** and phosphane sulfide **8**. Compound **8** was identified by ^{31}P NMR spectroscopy of the reaction mixture, and complex **7b** could be detected by ESI-MS.

The final trinuclear complex could then be produced via a tetranuclear complex formed from **7a** and **7b**. Reaction of this tetranuclear species with excess phosphane ligand could

[a] Department of Organic Chemistry, Arrhenius Laboratory, Stockholm University,
10691 Stockholm, Sweden
Fax: +46-8-154908
E-mail: bjorn.akermark@organ.su.se
[b] Division of Structural Chemistry, Arrhenius Laboratory, Stockholm University,
10691 Stockholm, Sweden
[c] Applied Electrochemistry, School of Science and Chemical Engineering, Royal Institute of Technology (KTH),
10044 Stockholm, Sweden
[d] Department of Organic Chemistry, Royal Institute of Technology (KTH),
10044 Stockholm, Sweden
[‡] Present address: School of Chemical Biology and Biotechnology,
Peking University Campus, Shenzhen University Town, China
Supporting information for this article is available on the WWW under http://dx.doi.org/10.1002/ejic.201000872.

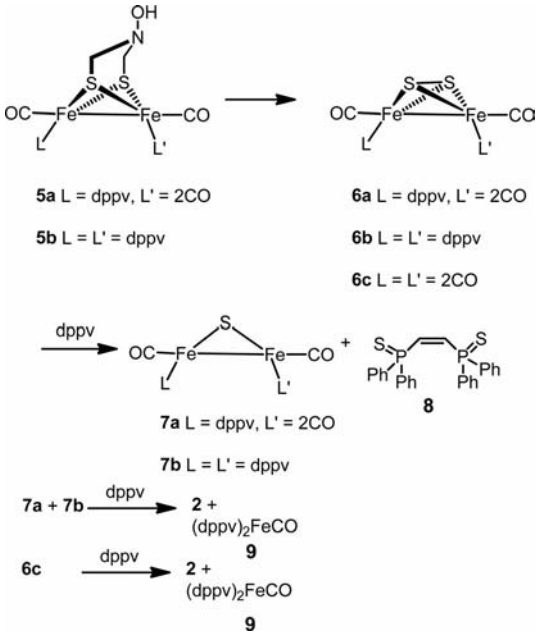

Scheme 2. Tentative mechanism for the formation of **2**.

then provide trinuclear complex **2** after elimination of one iron centre as mononuclear complex **9**, which could be detected by ESI-MS. Control experiments showed that complex **2** could also be obtained in approximately 49% yield from treatment of **6c** with dppv in toluene heated at reflux.

Related trinuclear FeS clusters containing only carbonyl ligands have previously been prepared in low yield by the reduction of iron pentacarbonyl with sulfite[6] and in approximately 50% yield from the reaction between triiron dodecacarbonyl and ethylene sulfide.[7] A trinuclear tris(triphenylphosphane) complex has also recently been prepared in approximately 30% yield by the treatment of disulfide **6c** with $LiEt_3BH$ in the presence of triphenylphosphane and $CuCl{\cdot}PPh_3$ or $AgNO_3{\cdot}PPh_3$.[8]

On protonation[9–13] with excess triflic acid in CH_2Cl_2 solution, complex **2** gave the bridged hydride species **3**. Complexes **2** and **3** were characterized by IR and NMR spectroscopy and CV studies. The IR spectrum of **2** in CH_2Cl_2 showed strong absorptions at 1997, 1943 and 1914 cm^{-1}, while for **3** four carbonyl absorptions appeared at 2090, 2050, 2032 and 1974 $cm.^{-1}$ This corresponds to an average shift $\Delta\nu$(CO) of 86 cm^{-1} upon protonation, which is in accordance with previous observations for dinuclear iron complexes.[3]

The solid-state structures of complexes **2** and **3** were established by X-ray crystallography. In the solid-state structure of **2** (Figure 1), the phosphorus atoms P1 and P2 both occupy basal (ba) positions, while in the second ligand P3 is in a ba position and P4 is in an apical (ap) position. This also appears to be the major conformation in solution, as suggested by the ^{31}P NMR spectra of complex **2** (Figure 2).

At room temperature, two signals of equal intensity were observed at δ = 97.3 and 66.4 ppm. According to a recent study of the dinuclear complex $[Fe_2(S_2C_3H_6)(CO)_4(dppv)]$,[3] the signal at δ = 66.4 ppm should correspond to

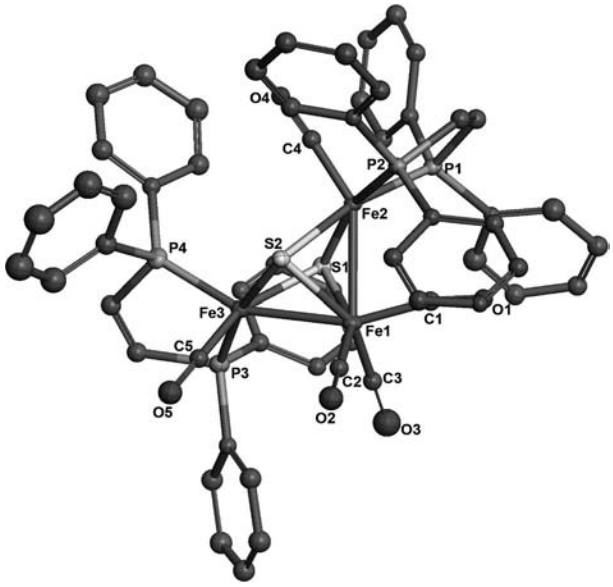

Figure 1. Structure of **2** showing 90% thermal ellipsoids. Selected bond lengths [Å] and angles [°]: Fe1–Fe2 2.600(2), Fe1–Fe3 2.591(2), Fe2–P1 2.217(3), Fe2–P2 2.207(3), Fe3–P3 2.193(3), Fe3–P4 2.149(4), P2–Fe2–P1 87.01(12), P4–Fe3–P3 87.31(12).

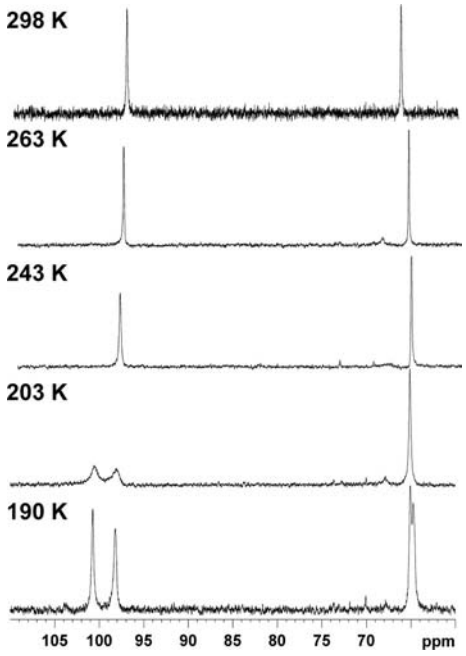

Figure 2. ^{31}P NMR spectra of complex **2**.

the two nearly equivalent phosphorus atoms P1 and P2. The signal at 97.3 ppm should thus originate from equilibrating phosphorus atoms P3 and P4. This was clearly shown when the spectra were run at lower temperatures. At 243 K, the signal at δ = 97.3 ppm broadened slightly and its intensity decreased by approximately 3% relative to the signal at δ = 66.4 ppm. At even lower temperature (203 K), three singlets were found at 100.6 and 97.4 and 65.1 ppm with an intensity ratio of 1:1:2. A reasonable explanation for this behaviour is that the phosphorus atoms P3 and P4

of the second ligand are in fast exchange by turnstile rotation at 298 K, but at 203 K the exchange is sufficiently slow to give rise to separate signals (Figure 2). Turnstile rotation also appears to take place for P1 and P2, but splitting of the signal at δ = 66.4 ppm into a partly overlapping doublet was observed only at 190 K. The difference in the fluxional behaviour of the dppv ligands is perhaps due to the reduced steric hindrance around the P1–P2 ligand. Alternatively, it might be more difficult to observe the splitting here because the P1–P2 chemical shift difference is small.

After protonation of **2**, the solid-state structure of the major isomer obtained corresponds to that of **3**, in which protonation of the Fe2–Fe3 bond has occurred (Figure 3, Scheme 1). Careful examination of the crystals, however, reveals a 30% contribution from a second structure, **4**, in which the alternative Fe–Fe bond has been protonated. The presence of compounds with differing Fe–H–Fe bonds can be confirmed from the IR spectrum, which shows an absorption pattern that is quite close to that of the reported μ-hydride derivative [Fe_2(μ-pdt)$(CO)_4$(dppe)(μ-H)] (dppe = $PPh_2CH_2CH_2PPh_2$).[3]

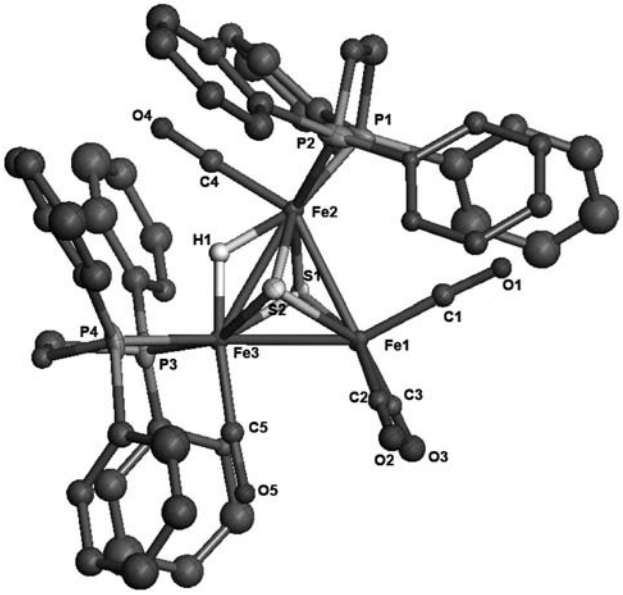

Figure 3. Structure of **3** showing 90% thermal ellipsoids. Selected bond lengths [Å] and angles [°]: Fe1–Fe2 2.6731(13), Fe1–Fe3 2.5811(12), Fe2–Fe3 2.7307(13), Fe2–P1 2.252(4), Fe2–P2 2.359(4), Fe3–P3 2.274(4), Fe3–P4 2.273(4), P2–Fe2–P1 83.38(9), P4–Fe3–P3 85.37(9).

Protonation of **2** to give **3** resulted in an increase of the Fe1–Fe2 distance by 0.078 Å, while the Fe1–Fe3 bond was shortened by 0.007 Å. As in **2**, one phosphane ligand in **3** occupies a ba-ba position, while the other is, in principle, coordinated ap-ba. In this ligand, the dihedral angle formed by the P3–Fe3–Fe1 and P4–Fe3–Fe1 planes was changed from 141.56 to 169.39°, making P3 and P4 essentially equivalent.

Other characteristic changes that were observed upon the protonation of **2** include the compression of the P2–Fe2–P1 angle from 87.01 to 83.09° and the elongation of the Fe2–P2 bond by 0.13 Å. The remaining distances and angles within the structure were essentially unaffected. The resulting geometry around the iron atoms can be described as two connected and distorted square pyramids in which the oxidation states of the iron atoms are Fe^{I}–Fe^{II}–Fe^{I} for **2** and Fe^{II}–Fe^{II}–Fe^{II} for **3**. The crystal structure of isomer **4** is not very accurate, but it is clear that protonation occurs at the Fe1–Fe2 bond, as shown by the elongation of this bond by approximately 0.07 Å.

At room temperature, the ^{31}P NMR spectrum of the mixture obtained upon protonation of complex **2** (Figure 4) is dynamic and broad, but at lower temperatures the signals become sharp. At 190 K, the major product **3** exhibited two or possibly three signals at δ = 86.2 and 73.7 ppm and perhaps also at δ = 86.0 ppm. We tentatively suggest that the signals at 86.2 and 86.0 ppm are derived from P3 and P4 of the formally ap-ba ligand, since the resonance at 86.2 ppm weakly correlates with the hydride signal at –13.0 ppm in the ^{1}H NMR spectrum. This is the major resonance in the hydride region of the ^{1}H NMR spectrum and appears as a triplet (J_{PH} = 27.1 Hz) because P3 and P4 become essentially equivalent upon protonation.

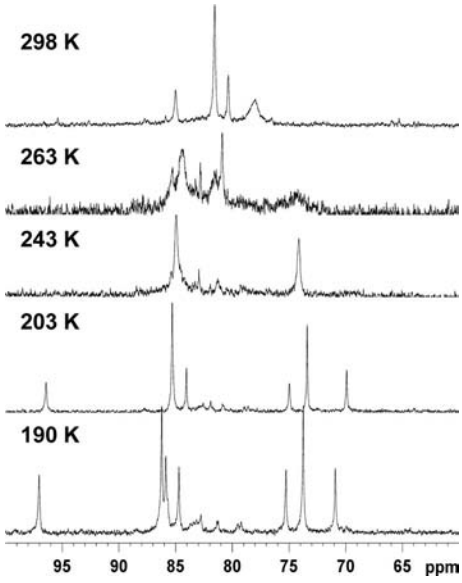

Figure 4. Variable-temperature ^{31}P NMR spectra of the mixture obtained from protonation of complex **2** in CD_2Cl_2 solution.

Since the second isomer **4** also gives a triplet in the ^{1}H NMR spectrum (Figure 5), one ligand must have the arrangement of P1 and P2 that is depicted in Scheme 3. Again, the ^{31}P NMR spectrum, which was dynamic at 298 K, sharpened to four signals at 190 K. Since the peaks at δ = 97 and 75 ppm seem to belong together, and also those at δ = 85 and 71 ppm, we tentatively suggest that a 1:1 equilibrium between the symmetric structures **4** and **4′** is formed in solution (Scheme 3, Figure 4). In addition, the ^{1}H NMR spectrum suggests that two minor isomers appear to form in the reaction; **3′**, as shown by a triplet at –9.4 ppm (J_{PH} = 46.7 Hz), and **4′′**, as suggested by the doublet at –10.7 ppm (J_{PH} = 19.4 Hz) (Scheme 3, Figure 5).

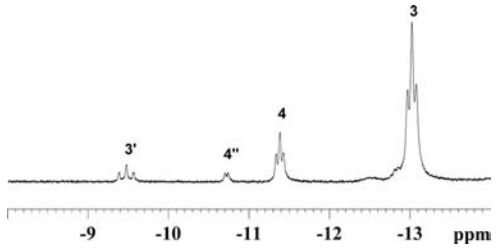

Figure 5. The metal hydride signals in the ^{1}H NMR spectrum of the mixture obtained from protonation of **2** at 298 K.

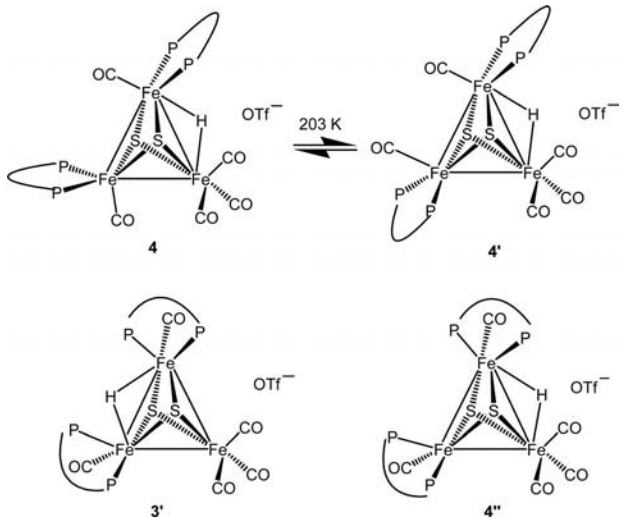

Scheme 3. Additional structures formed upon protonation of **2**.

Cyclic voltammetry studies of complex **2** were performed at different concentrations of triflic acid. Without triflic acid, the potentials for the oxidation peaks of complex **2** ($Fe^IFe^{II}Fe^I/Fe^{II}Fe^{II}Fe^I$ and $Fe^{II}Fe^{II}Fe^I/Fe^{II}Fe^{II}Fe^{II}$) were found at –0.27 and 0.05 V, respectively, and the first reduction peak ($Fe^IFe^{II}Fe^I/Fe^IFe^IFe^I$) was at –2.05 V (Figure 6).

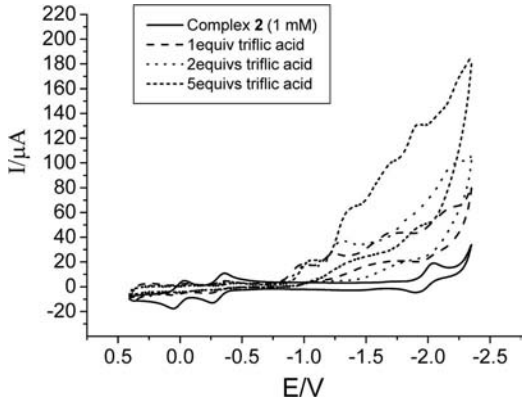

Figure 6. Cyclic voltammograms of complex **2** in 0.05 M nBu$_4$NPF$_6$/CH$_2$Cl$_2$ in the absence and presence of triflic acid (scan rate = 100 mV/s). Redox potentials are given vs. Fc^+/Fc unless otherwise indicated.

With the addition of acid, a sharp anodic shift, ΔE = 1007 mV, was observed and could be attributed to the protonation of one Fe–Fe bond. This shift is even greater than that reported for diprotonated adt [2Fe2S] model complexes (usually approximately 690 mV).[14–16] The first reduction peak appears at –0.98 V, which is quite close to the recently reported value for the triiron all carbonyl cluster (–1.03 V)[17] and also very close to the reduction potentials observed for [FeFe] hydrogenases in nature (–0.8 to –1.1 V, –0.4 to –0.7 V vs. NHE).[18] At this potential, however, the CV does not indicate any electrochemical activity upon addition of HOTf. In contrast, the current at the reduction peaks of **3** (–1.23 and –1.88 V) is sharply increased on addition of acid, which is indicative of hydrogen formation. All of the currents for the active reduction peaks displayed a first-order dependence on [HOTf] (see Supporting Information). Although protonation may require previous reduction of the catalyst,[19] it is nonetheless obvious that the first step in hydrogen formation is protonation, and thus a CECE (chemical-electrochemical-chemical-electrochemical) mechanism for this process seems reasonable.

The first redox potential of **2** after protonation (–0.98 V) is more positive than that of the excited sensitizer tris(bipyridine)ruthenium(II) {$[Ru(bpy)_3]^{2+*}$, ca. –1.11 V}. Mass spectrometry was therefore used to study if photoinduced formation of hydrogen could be observed upon irradiation of **2** with visible light.[1,20]

Hydrogen was initially formed when a mixture of $[Ru(bpy)_3]^{2+}$, **2**, and four equiv. of TfOH in acetonitrile solution containing a small amount of water was illuminated, but, as expected, the reaction stopped due to the absence of a sacrificial donor to reduce the formed Ru^{III} back to Ru^{II}. The addition of D_2O was used to show that water acted as the terminal proton source in this system (Figure 7).

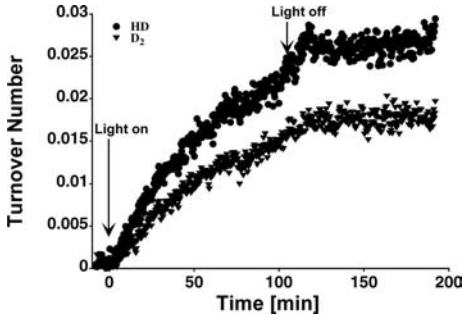

Figure 7. Light-induced hydrogen generation in the system including $[Ru(bpy)_3]^{2+}$ (2 μmol), [3Fe2S] (2 μmol), [HOTf] (8 μmol), CH_3CN (5 mL) and D_2O (0.15 mL).

The observed decrease in reaction rate is probably due to breakdown of the complex caused by loss of CO (approximately four molecules of CO were formed per molecule of complex). In the ESI-MS spectrum from a solution of the pure complex, one of the main peaks was at *m*/*z* 1136, which corresponds to the loss of one CO molecule, but there were no peaks corresponding to the loss of more than one CO, which suggests that the complex breaks down under these conditions. IR spectroscopic studies showed that essentially all of the catalyst was consumed after the irradi-

ation. It is interesting to note that the relative kinetics of CO and hydrogen formation were the same.

Exploratory experiments were performed in order to try to observe electron transfer from an excited $[Ru(bpy)_3]^{2+}$-type sensitizer to complex **2** in strongly acidic solution. Unfortunately, these experiments were inconclusive due to decomposition of the complex under the experimental conditions employed.[21]

Conclusions

We have successfully converted a dinuclear [2Fe2S] cluster to an asymmetric, trinuclear [3Fe2S] cluster **2**, which contains two bis(phosphane) ligands, in quite reasonable yield. The mechanism of this reaction is not clear and is being studied further. Upon protonation of **2**, hydride **3** is formed, which has unusually positive reduction potentials. Indeed, electrochemical reduction produces hydrogen at approximately –1.1 V.

Experimental Section

Unless otherwise indicated, all reactions were carried out under a dry, oxygen-free atmosphere of argon with standard Schlenk techniques. Chemicals were purchased from Aldrich, and all solvents were dried and distilled prior to use according to the standard methods.

Infrared spectra were recorded with a Perkin–Elmer spectrum 1 instrument. NMR spectra were collected with a Bruker Avance II spectrometer (500 MHz). The elemental analyses were performed in Analytische Laboratorien, Lindar, Germany. The mass spectrometry experiments were performed with a Bruker Daltonics BioAPEX-94e superconducting 9.4 tesla FTICR mass spectrometer (Bruker Daltonics, Billerica, MA, USA) (FTICR-ESI MS).

CH_2Cl_2 (Aldrich, spectroscopy grade) used for electrochemistry was dried with molecular sieves (4 Å) and then freshly distilled from CaH_2 under argon. A solution of nBu$_4$NPF$_6$ (0.05 M, Fluka, electrochemical grade) in CH_2Cl_2 was used as electrolyte. Electrochemical measurements were carried out in a three-electrode cell connected to an Autolab potentiostat with a GPES electrochemical interface. The working electrode was a glassy carbon disc (diameter 2 mm, freshly polished). The reference electrode was a nonaqueous Ag/Ag^+ electrode (1.0 mM $AgNO_3$ in CH_3CN) with the ferrocene/ferrocenium (Fc^+/Fc) couple as external standard. The auxiliary electrode was a platinum wire. All potentials reported here are quoted relative to the Fc^+/Fc couple or converted to values vs. SCE by subtraction of 400 mV. The solutions were purged with solvent-saturated argon to remove residual oxygen. All experimental measurements were kept under an atmosphere of argon at all times.

Complexes **1a** and **1b** were prepared according to an earlier report.[1] See also Supporting Information.

[Fe$_3$S$_2$(CO)$_5$(dppv)$_2$] (2) and [Fe$_2$S$_2$(CO)$_4$(dppv)] (6a): A solution of **1a** or **1b** (0.094 g, 0.2 mmol) and $Me_3NO{\cdot}2H_2O$ (0.022 g, 0.2 mmol) in CH_3CN (15 mL) was stirred at room temperature for 10 min, then dppv (0.079 g, 0.2 mmol) in toluene (20 mL) was added. After stirring at room temperature for 10 min, the solution was heated at 110 °C for 1 h. The solvent was removed on a rotary evaporator, and the crude product was purified by column chromatography with CH_2Cl_2/hexane/Et_3N (100:300:4 v/v/v) as eluent to give green solid complex **2** (107 mg, 51%) and red solid complex **6a** (7 mg, 5%). **2**: ^{1}H NMR (CD_2Cl_2): δ = 7.3–7.8 (m, 40 H, Ph) ppm. ^{31}P NMR (CD_2Cl_2, 25 °C): δ = 97.3 (s), 66.4 (s) ppm. IR (CH_2Cl_2): $\tilde{\nu}$ = 1997 (CO), 1943, 1919 cm^{-1}. $C_{57}H_{44}Fe_3O_5P_4S_2$ (1164.54): calcd. C 58.79, H 3.81; found C 59.07, H 4.02. **6a**: ^{1}H NMR (CD_2Cl_2): δ = 7.1–7.7 (m, 20 H, Ph) ppm. ^{31}P NMR (CD_2Cl_2, 25 °C): δ = 87.5 (s), 70.1 (s) ppm. IR (CH_2Cl_2): $\tilde{\nu}$ = 2015 (CO), 1971, 1933 cm^{-1}. $C_{30}H_{22}Fe_2O_4P_2S_2$ (684.26): calcd. C 52.66, H 3.24; found C 53.07, H 3.72.

Protonation Experiments: A solution of **2** (0.008 g, 0.01 mmol) in CH_2Cl_2 (0.5 mL) was treated with $HBF_4{\cdot}Et_2O$ (5 equiv.). The mixture was stirred for 10 min under argon, and then hexane (5 mL) was added to precipitate a brown red powder. The precipitate was washed twice with hexane (5 mL) and then dried in vacuo to give **3**. A single crystal was cultivated in hexane/CH_2Cl_2 solution at room temperature.

3: ^{1}H NMR (CD_2Cl_2): δ = 7.3–8.0 (m, 40 H, Ph), –11.3 (t, J_{PH} = 23.4 Hz, 0.2 H, Fe-H-Fe), –13.0 (t, J_{PH} = 27.1 Hz, 0.8 H, Fe-H-Fe) ppm. ^{31}P NMR (CD_2Cl_2, 25 °C): δ = 85.0 (s), 81.5 (s), 80.3 (s), 78.1 (s) ppm. IR (CH_2Cl_2): $\tilde{\nu}$= 2090 (CO), 2050, 2032, 1974 cm^{-1}. $C_{57}H_{45}BF_4Fe_3O_5P_4S_2$ (1252.34): calcd. C 54.67, H 3.62; found C 54.91, H 3.89.

Single-crystal X-ray diffraction patterns were recorded with an Oxford Diffraction Excalibur diffractometer equipped with a sapphire-3 CCD on a Moradiation source (λ = 0.71073 Å) with ω-scans at different ϕ values to fill the Ewald sphere. The sample–detector distance was 50 mm. The maximum 2θ was approximately 63°.

Indexing, cell refinements and integration of reflection intensities were performed with the CrysAlis software.[22] Numerical absorption correction was performed with the program X-RED[23] verifying the crystal shape with program X-shape[24] The structure was solved by direct methods using SHELXS97,[25] giving electron density maps where most of the non-hydrogen atoms could be resolved. The remaining non-hydrogen atoms were located from difference electron density maps, and the structure model was refined with full-matrix least square calculations on F^2 using the program SHELXL97-2.[26]

All non-hydrogen atoms were refined with anisotropic displacement parameters and hydrogen atoms, which were placed at geometrically calculated positions and let to ride on the atoms they were bonded to, were given isotropic displacement parameters calculated as $\xi{\cdot}U_{eq}$ for the non-hydrogen atoms with ξ = 1.2 for methylene (–CH_2–) and aromatic hydrogen atoms. CCDC-751212 (**2**) and -751213 (**3**) contain the supplementary crystallographic data for this paper. These data can be obtained free of charge from The Cambridge Crystallographic Data Centre via www.ccdc.cam.ac.uk/data_request/cif.

Supporting Information (see footnote on the first page of this article): Bond lengths and bond angles of **2** and **3**, reduction current of **3** vs. (scan rate)$^{1/2}$, CV of **2** + acid, setup for oxygen determination.

Acknowledgments

We are grateful to the Swedish Research Council, K&A Wallenberg Foundation and the Swedish Energy Agency for financial support of this work.

[1] W. Gao, J. Sun, T. Åkermark, M. Li, L. Eriksson, L. Sun, B. Åkermark, *Chem. Eur. J.* **2010**, *16*, 2537–2546.

[2] A. K. Justice, G. Zampella, L. De Gioia, T. B. Racufuss, J. I. van der Vlugt, S. R. Wilson, *Inorg. Chem.* **2007**, *46*, 1655–1664.
[3] S. Ezzaher, J.-F. Capon, F. Gloaguen, F. Y. Pétillon, P. Schollhammer, J. Talarmin, *Inorg. Chem.* **2007**, *46*, 3426–3428.
[4] W. Gao, J. Ekström, J. Liu, C. Chen, L. Eriksson, L. Weng, B. Åkermark, L. Sun, *Inorg. Chem.* **2007**, *46*, 1981–1991.
[5] A. C. Cope, N. A. Lebel, H. H. Lee, W. R. Moore, *J. Am. Chem. Soc.* **1957**, *79*, 4720–4729.
[6] a) W. Huber, J. Gruber, *Z. Anorg. Allg. Chem.* **1958**, *296*, 91–103; b) T. M. Bockman, J. K. Kochi, *J. Am. Chem. Soc.* **1987**, *109*, 7725–7735.
[7] R. D. Adams, J. E. Babin, *Inorg. Chen.* **1986**, *25*, 3418–3422.
[8] B. Zhuang, J. Chen, L. He, J. Chen, Z. Zhou, K. Wu, *J. Organomet. Chem.* **2004**, *689*, 2674–2683.
[9] X. Zhao, I. P. Georgakaki, M. L. Miller, R. Mejia-Rodriguez, C. Chiang, M. Y. Darensbourg, *Inorg. Chem.* **2002**, *41*, 3917–3928.
[10] A. K. Justice, T. B. Rauchfuss, S. R. Wilson, *Angew. Chem. Int. Ed.* **2007**, *46*, 6152–6154.
[11] A. K. Justice, M. J. Nilges, T. B. Rauchfuss, S. R. Wilson, L. De Gioia, G. Zampella, *J. Am. Chem. Soc.* **2008**, *130*, 5293–5301.
[12] B. E. Barton, T. B. Rauchfuss, *Inorg. Chem.* **2008**, *47*, 2261–2263.
[13] A. K. Justice, G. Zampella, L. De Gioia, T. B. Rauchfuss, *Chem. Commun.* **2007**, 2019–2021.
[14] G. Eilers, L. Schwartz, M. Stein, G. Zampella, L. De Gioia, S. Ott, R. Lomoth, *Chem. Eur. J.* **2008**, *13*, 7075–7084.
[15] F. Wang, M. Wang, X. Liu, K. Jin, W. Dong, L. Sun, *Dalton Trans.* **2007**, 3812–3819.
[16] J.-F. Capon, S. Ezzaher, F. Gloaguen, F. Y. Pétillon, P. Schollhammer, J. Talarmin, *Chem. Eur. J.* **2008**, *14*, 1954–1964.
[17] Z. Li, X. Zeng, Z. Niu, X. Liu, *Electrochim. Acta* **2009**, *54*, 3638–3644.
[18] C. M. Thomas, O. Rüdiger, T. Liu, C. E. Carson, M. B. Hall, M. Y. Darensbourg, *Organometallics* **2007**, *26*, 3976–3984.
[19] G. A. N. Felton, A. K. Vannucci, J. Chen, T. Lockett, N. Okumura, B. J. Petro, U. I. Zakai, D. H. Evans, R. S. Glass, D. L. Lichtenberger, *J. Am. Chem. Soc.* **2007**, *129*, 12521–12530.
[20] T. Åkermark, B. Emmoth, H. Bergsåker, *J. Nucl. Mater.* **2006**, *359*, 220–226.
[21] We thank Prof B. Albinsson and Dr J. Wiberg for these measurements.
[22] Oxford Diffraction Ltd., Xcalibur CCD system, CrysAlis Software system, Version 1.170, **2003**.
[23] *X-RED*, *Absorption Correction Program*, version 1.09, Stoe & Cie GmbH Darmstadt, Germany.
[24] *X-SHAPE*, *Crystal Optimisation for Numerical Absorption Correction*, version 1.2, Stoe & Cie GmbH Darmstadt, Germany.
[25] G. M. Sheldrick, *Acta Crystallogr., Sect. A* **1990**, *46*, 467.
[26] G. M. Sheldrick, Computer *Program for the Refinement of Crystal Structures*, Göttingen, Germany, **1997**.

Received: August 13, 2010
Published Online: January 5, 2011

